

Microstructure and Properties of Metal Infiltrated RBSN Composites

Nahum A. Travitzky* & Nils Claussen†

Technische Universität Hamburg-Harburg, Advanced Ceramics Group, D-2100 Hamburg 90, FRG

(Received 23 October 1990; revised version received 6 May 1991; accepted 10 May 1991)

Abstract

Reaction-bonded silicon nitride (RBSN)–metal composites were fabricated using gas-pressure infiltration. Various RBSN types have been infiltrated with molten Al, an Al–Si–Mg alloy, a Ti–Al intermetallic, and Si, resulting in considerable increase in mechanical properties when compared to uninfiltrated RBSN. For example, strength was raised to 510 from 227 MPa when infiltrated with a Ti–39 wt% Al alloy and the toughness to >5 from $2.7 \text{ MPa}\sqrt{\text{m}}$ when pure Al was infiltrated. Si infiltration proved to be most effective in enhancing the wear resistance.

Reaktionsgebundenes Siliciumnitrid (RBSN) wurde unter Gasdruck mit reinem Aluminium, einer Al–Si–Mg-Legierung, einer Ti–Al-Legierung und mit Silicium infiltriert. In allen Fällen wurden die mechanischen Eigenschaften von RBSN z. T. erheblich verbessert. Beispielsweise konnte die Festigkeit von 227 auf 510 MPa durch eine 39 Gew% Al-haltige Ti-Legierung und die Bruchzähigkeit von 2.7 auf $>5 \text{ MPa}\sqrt{\text{m}}$ durch reines Aluminium gesteigert werden. Silicium erwies sich zur Verbesserung des Verschleißwiderstandes am besten geeignet.

On a élaboré des composites Si_3N_4 (RBSN)–métal par infiltration sous pression de gaz. Différents types de RBSN ont été infiltrés par de l'aluminium fondu, un alliage Al–Si–Mg, un intermétallique Ti–Al et enfin par du silicium, conduisant à des matériaux ayant des propriétés mécaniques considérablement améliorées. L'infiltration par un alliage Ti–39 wt% Al permet par exemple de faire passer la résistance mécanique de 227 à 510 MPa tandis que la ténacité passait de 2.7 à

$>5 \text{ MPa}\sqrt{\text{m}}$ pour une infiltration par de l'Al pur. L'infiltration par du silicium s'est avérée être la plus efficace pour améliorer la résistance à l'usure.

1 Introduction

Ductile metal reinforcements considerably increase the fracture toughness of ceramic materials. The dominant toughening mechanism in this case results from bridging of the extending crack by the plastically deforming metal behind the crack tip.^{1–5} Several processing methods have been used to produce metal-reinforced ceramic composites.^{4,6–9} One of the preferred techniques to fabricate ceramic–metal composites, where the inherent properties of the ceramic dominate the overall properties, is pressureless infiltration of a porous ceramic with a liquid metal which has to wet the ceramic phase. This is the case for most carbides, e.g. Si–SiC composites can easily be made by infiltration processing.¹⁰ Problems usually arise with oxides and nitrides where either the wettability by the metal must be improved, e.g. by alloying, or pressure has to be applied during the infiltration.¹¹

Reaction-bonded silicon nitride (RBSN) typically exhibits porosities of $>15\%$, mainly as open porosity. It is hence desirable for some applications to fill the pores with a metal phase in order to improve mechanical and surface properties. Leimer & Gugel¹² and Schmidt¹³ tried to infiltrate RBSN with a number of metal alloys. However, in spite of reasonable wettability by some alloys, infiltration could only be observed when reactions with the Si_3N_4 matrix took place. This was essentially the case for Si and Mg alloys with high Ca content. However, the mechanical properties of infiltrated and reacted RBSN composites were hardly im-

* Present address: Materials Department, University of Tel Aviv, Israel.

† To whom correspondence should be addressed.

proved when compared to the uninfiltreated RBSN matrix.

In this work, a gas-pressure technique was successfully applied to infiltrate various RBSN types with molten aluminum, an aluminum alloy, a titanium–aluminum intermetallic compound and silicon.

2 Experimental

RBSN ceramics with open porosities of ~18% (Annawerk, Rödentel, FRG, pore size distribution given in Fig. 1), ~15% (Hoechst CeramTec, Selb, FRG) and ~25% (Iscar, Naharia, Israel) and average pore diameters of 0.16 μm , 0.1 μm and 0.25 μm , respectively, were infiltrated with Al (99.9%; VAW, Bonn, FRG), Al alloy (2.5 wt% Mg, 5 wt% Si, 1 wt% Zn; VAW), Ti–39 wt% Al intermetallic (Kobe Steel, Kobe, Japan) and Si (99.99%; H. C. Starck, Berlin, FRG).

A schematic diagram of the gas-pressure infiltration technique applied is shown in Fig. 2. RBSN bodies to be infiltrated were mechanically fixed at the bottom of an Al_2O_3 crucible and covered with a metal plate. Then, the system was heated in a gas-pressure furnace under vacuum to a temperature above the melting point of the metal (Al and Al alloy to between 775 and 900°, Ti–39 wt% Al and Si to 1575°). The application of an Ar gas pressure between 5 and 80 bar for 5 min forced the molten metal to infiltrate the RBSN samples. On cooling, application of pressure was continued until solidification of the melt occurred. An Al-infiltrated

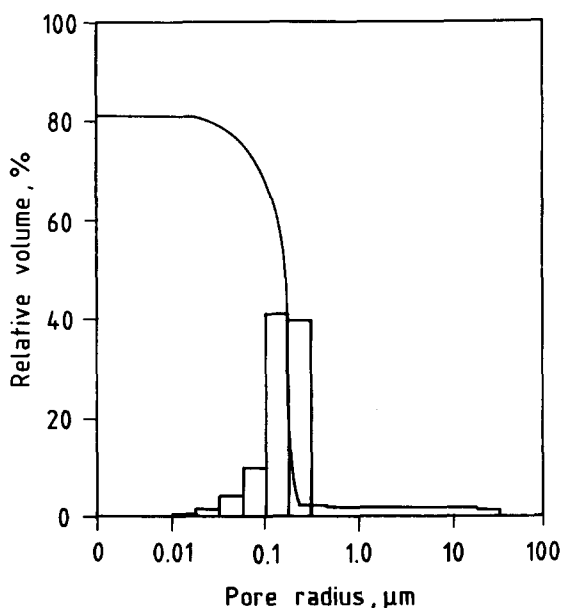


Fig. 1. Pore size distribution of Annawerk RBSN (Micromeritics Mercury Porosimeter).

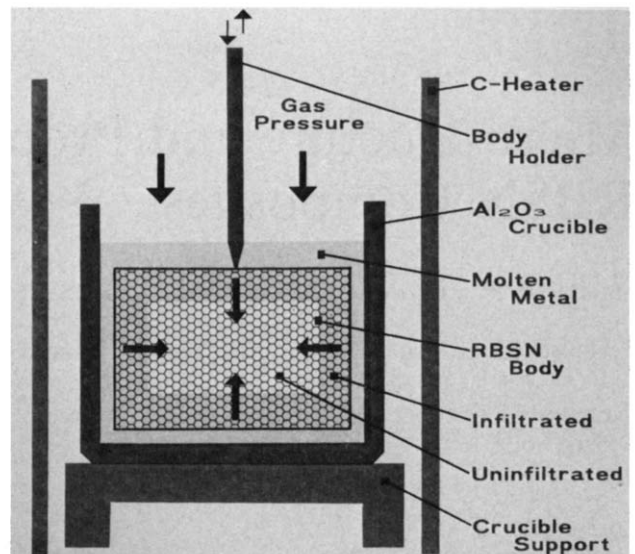


Fig. 2. Schematic diagram of gas-pressure infiltration of RBSN.

RBSN was annealed for 12 h in both air and N_2 at ambient pressure.

Bending strength of uninfiltreated and infiltrated bars (3 mm \times 4 mm \times 34 mm) was measured by four-point bending using spans of 30 and 10 mm. Fracture toughness was measured by the indentation strength in bending (ISB) technique.¹⁴ The indented samples (load 100 N) were broken in three-point bending with a 16 mm span. The tensile surface of the samples was polished to a 1 μm finish. The crosshead speed was 10 $\mu\text{m min}^{-1}$ in all cases. For comparison, the fracture toughness by the indentation crack length (ICL) technique¹⁵ was also determined. The Vickers microhardness was measured for all samples using a load of 100 N. Wear properties of uninfiltreated and infiltrated samples (3 mm \times 4 mm \times 4.5 mm) were measured using a pin-on-disc technique with 180 mesh (70 μm) and 600 mesh (15 μm) SiC papers.¹⁶ The composites were analyzed by XRD, SEM and optical microscopy.

3 Results and Discussion

3.1 Infiltration of RBSN with molten metals

Nearly complete infiltration of all RBSN types with Al and Al alloy was obtained at pressures ≥ 40 bar applied for 5 min at 900°C. The threshold pressure P which is necessary to move the molten metal along the pores depends on the surface tension of molten metal γ , the wetting angle Θ and pore diameter d :¹⁷

$$P = -\frac{4\gamma \cos \Theta}{d} \quad (1)$$

For example, for the infiltration of pure Al ($\gamma = 1 \text{ J}$

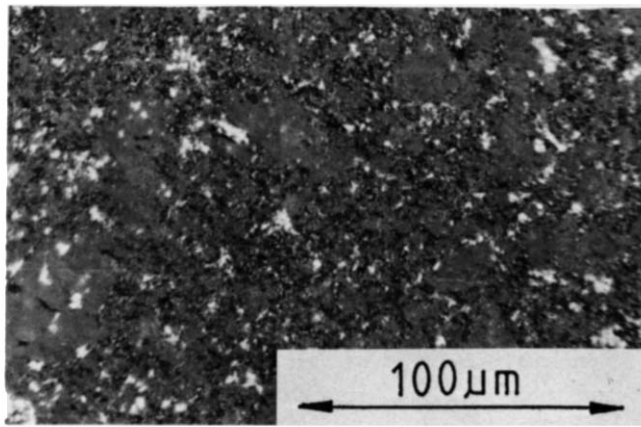
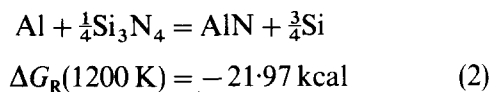


Fig. 3. Microstructure of Al alloy-infiltrated RBSN (Annawerk).

m^{-2})¹⁸ into RBSN (Annawerk, $d \approx 0.16 \mu m$) at $900^\circ C$ ($\Theta = 110^\circ$)¹⁹ a threshold pressure at 85 bar would be necessary. The difference between the values of applied and calculated pressure is partially due to a chemical reaction between the molten Al and the RBSN¹⁹ according to:



The reaction results in a change of the interfacial free energy and thus the wetting angle. Hence, chemical reaction between Al and RBSN enhances the infiltration. Long-time exposure of RBSN in molten Al, however, can result in a considerable change of the phase composition and in formation of Si_3N_4/AlN or AlN -based composites. In the case of RBSN with micropores $< 0.1 \mu m$, reaction products can prevent further infiltration of the molten Al when the reaction rate is higher than the rate of pressure increasing to the infiltration level. This was true for an experimental fine-porosity ($< 0.05 \mu m$) RBSN supplied by NGK Insulators, Nagoya.

3.2 Microstructure

The microstructure of Al-alloy infiltrated RBSN (Annawerk) is shown in Fig. 3. Similar microstructures were observed for all RBSN-metal composites.

XRD analyses of all uninfiltrated RBSN samples showed the presence of α - and β - Si_3N_4 . For Al-infiltrated RBSN (Annawerk), the additional phases that could be detected next to Si_3N_4 and Al were AlN and Si. Traces of AlN, Si and Mg_2Si were detectable in RBSN-Al alloy composites. Traces of TiN and Ti_5Si_3 could be observed in RBSN-Ti-39 wt% Al composites next to Si_3N_4 , TiAl and Ti_3Al . XRD analysis of the RBSN-Si composites only showed the presence of α -, β - Si_3N_4 and Si.

RBSN (Annawerk)-Al samples annealed in air and N_2 at $1200^\circ C$ did not show any sweating out of Al. Rather Al_2O_3 or AlN, respectively, formed to seal off the surface channels.

3.3 Mechanical properties

The mechanical properties of infiltrated RBSN-metal composites are compiled in Table 1. In all cases, the properties of infiltrated RBSN are considerably improved. Al and Al alloy especially enhance the fracture toughness, while Ti-39 wt% Al intermetallic improves bending strength and hardness of RBSN from 227 to 510 MPa and from 5.1 to 15.3 GPa, respectively.

The less porous RBSN (Hoechst CeramTec) exhibits an even greater hardness increase when infiltrated with the Al alloy. The opposite effect is shown by the high-porosity RBSN (Iscar).

Fig. 4 shows the influence of infiltration pressure on mechanical properties of RBSN (Annawerk)-Al alloy composites. From gas pressures > 10 bar, bending strength, fracture toughness and Vickers hardness increase with pressure. This is due to

Table 1. Mechanical properties of metal-infiltrated RBSN

Material	Bending strength (MPa)	Fracture toughness (MPa \sqrt{m})		Hardness HV 10 (100N)	
		ISB	ICL		
RBSN (Annawerk)	Not infiltrated	227 \pm 15	2.70 \pm 0.15	—	510
	Al alloy	450 \pm 18	4.52 \pm 0.11	5.23 \pm 0.15	1170
	Al (99.9%)	478 \pm 15	5.00 \pm 0.20	5.58 \pm 0.14	1100
	Si (99.99%)	427 \pm 20	3.90 \pm 0.20	4.74 \pm 0.11	1530
	Ti-39 wt% Al	510 \pm 20	n.m.	4.90 \pm 0.50	1524
RBSN (Hoechst)	Not infiltrated	n.m.	n.m.	—	550
	Al alloy	n.m.	n.m.	5.00 \pm 0.08	1340
RBSN (Iscar)	Not infiltrated	n.m.	n.m.	—	216
	Al alloy	n.m.	n.m.	4.15 \pm 0.10	900
	Si (99.99%)	n.m.	n.m.	3.60 \pm 0.20	960

n.m. = not measured.

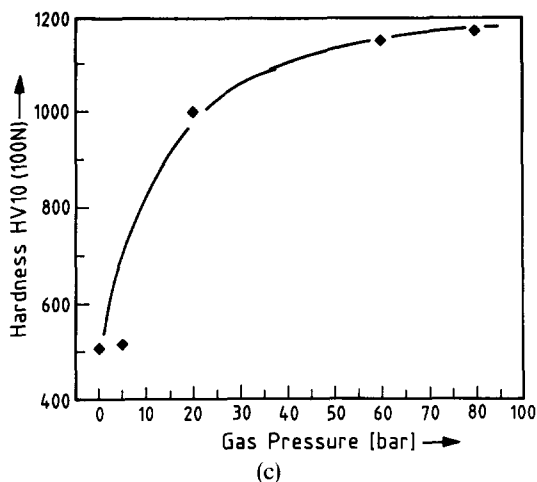
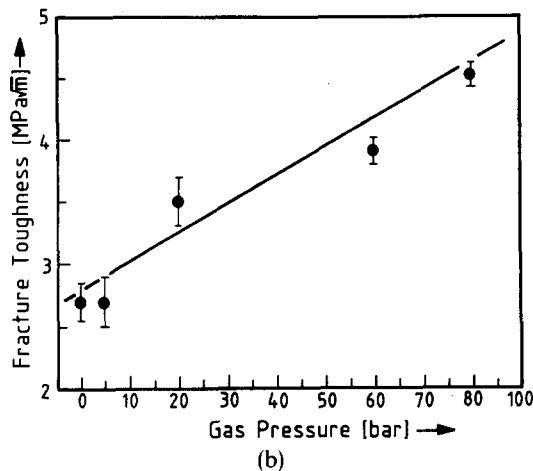
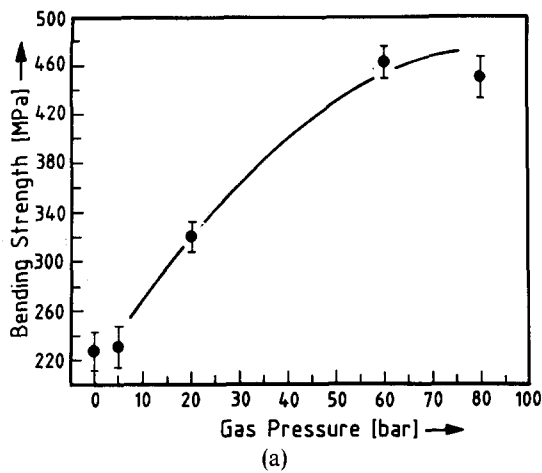


Fig. 4. Influence of the infiltration pressure on (a) bending strength, (b) fracture toughness and (c) hardness of RBSN–Al alloy composites.

increased filling of the pores. Application of pressures ≥ 40 bar resulted in a twofold improvement in mechanical properties of the composites when compared to the uninfiltrated material.

The toughness increase of RBSN–Al, RBSN–Al alloy or RBSN–Ti–39 wt% Al composites is clearly related to crack bridging by the ductile phase, as demonstrated in Fig. 5(a). The dominant contribution to the fracture toughness is the plastic deformation of the ligaments as demonstrated in

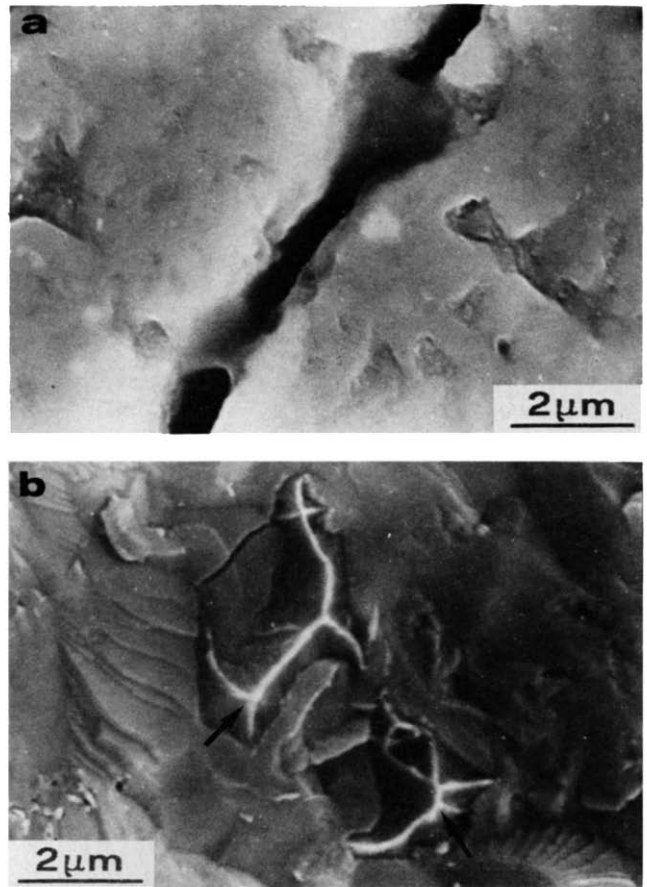


Fig. 5. (a) Bridging Al ligaments and (b) fracture surface of such ligaments in RBSN (Annawerk)–Al composite. Al has plastically deformed to sharp edges (arrows).

Fig. 5(b). The Al phase has necked down to sharp edges (see arrows in Fig. 5(b)).

The enhanced properties of RBSN–Si partially explained by the microstress concept.^{20,21} Compressive residual microstresses are generated in the weak Si phase resulting mainly from the relative volume increase of Si on solidification. Wear resistance to SiC (180 mesh) paper abrasion increased up to a factor of 7 when Si was infiltrated into Annawerk RBSN.¹⁶

4 Conclusions

Gas pressures >40 bar are necessary to fully infiltrate RBSN with Al, Al alloys and Si. Strength, toughness, hardness and wear resistance are considerably improved when compared to the matrix material. Crack bridging is the dominant toughening mechanism for the Al- and Al alloy-containing RBSN, while residual microstresses are thought to be the major contributing mechanism in RBSN–Si composites. It is assumed that surface sealing of infiltrated RBSN by air or N_2 annealing will further improve the wear resistance.

Acknowledgement

The authors thank the Deutsche Forschungsgemeinschaft (DFG) for financial support under contract No. Cl 52/10.

References

1. Sigl, L. S., Mataga, P. A., Dalgleish, B. J., McMeeking, R. M. & Evans, A. G., On the toughness of brittle materials reinforced with a ductile phase. *Acta Metall.*, **36**(4) (1988) 945–53.
2. Budiansky, B., Amazigo, J. C. & Evans, A. G., Small-scale crack bridging and the fracture toughness of particulate-reinforced ceramics. *J. Mech. Phys. Solids*, **36**(1988) 167–87.
3. Flinn, B. D., Rühle, M. & Evans, A. G., Toughening in composites of Al₂O₃ reinforced with Al. *Acta Metall.*, **37**(11) (1989) 3001–6.
4. Krstic, V. V., Nicholson, P. S. & Hoagland, R. G., Toughening of glasses by metallic particles. *J. Am. Ceram. Soc.*, **64**(9) (1981) 499–504.
5. Andersson, C. A. & Aghajanian, M. K., The fracture toughening mechanism of ceramic composites containing adherent ductile metal phases. *Ceram. Eng. Sci. Proc.*, **9**(7–8) (1988) 621–6.
6. Kieffer, B. & Benesovsky, F., *Hartmetalle*, Springer-Verlag, Vienna, 1965.
7. Newkirk, M. S., Leshner, H. D., White, D. R., Kennedy, C. R., Urquhart, A. W. & Claar, T. D., Preparation of Lanxide™ ceramic matrix composites: matrix formation by the direct oxidation of molten metals. *Ceram. Eng. Sci. Proc.*, **8**(7–8) (1987) 879–90.
8. Lange, F. F., Velamakanni, B. V. & Evans, A. G., Method for processing metal-reinforced ceramic composites. *J. Am. Ceram. Soc.*, **73**(2) (1990) 388–93.
9. Claar, T. D., Johnson, W. B., Andersson, C. A. & Schiroky, G. H., Microstructure and properties of platelet-reinforced ceramics formed by the directed reaction of zirconium with boron carbide. *Ceram. Eng. Sci. Proc.*, **10**(7–8) (1989) 599–609.
10. Kieffer, R., Eipeltauer, E. & Gugel, E., New in the field of cermets. *Ber. Dt. Keram. Ges.*, **46** (1969) 486–92.
11. Jangg, V. G., Kieffer, R., Gugel, E., Kollwentz, W. & Jicinsey, G., Application of the infiltration technique to the manufacture of cermets. *Ber. Dt. Keram. Ges.*, **48** (1971) 262–8.
12. Leimer, G. & Gugel, E., Composite materials by infiltration of silicon nitride. *Z. Metallkde.*, **66** (1975) 570–6.
13. Schmidt, W. G., Metallic infiltration of reaction bonded silicon nitride. *Progress in Nitrogen Ceramics*, ed. F. L. Riley. Martinus Nijhoff Publishers, Boston, USA, pp. 447–53.
14. Chantikul, P., Anstis, G. R., Lawn, B. R. & Marshall, D. B., A critical evaluation of indentation techniques for measuring fracture toughness: II: Strength Method. *J. Am. Ceram. Soc.*, **64**(9) (1981) 539–43.
15. Anstis, G. R., Chantikul, P., Lawn, B. R. & Marshall, D. B., A critical evaluation of indentation techniques for measuring fracture toughness: I. Direct crack measurements. *J. Am. Ceram. Soc.*, **64**(9) (1981) 533–9.
16. Holz, D., Janssen, R., Friedrich, K. & Claussen, N., Abrasive wear of ceramic-matrix composites. *J. Eur. Ceram. Soc.*, **5** (1989) 229–32.
17. Washburn, E. W., Note on a method of determining the distribution of pore sizes in a porous material. *Proc. Natl Acad. Sci.*, **7** (1921) 115–16.
18. Dellanay, F., Froyen, L. & Deruttere, A., The wetting of solids by molten metals and its relation to the preparation of metal-matrix composites. *J. Mat. Sci.*, **22** (1987) 1–16.
19. Loehman, R. E., Joining and bonding mechanisms in nitrogen ceramics. In *Proc. Int. Meeting, Metal-Ceramic Joints*, ed. Masao Doyama, MRS, Pittsburgh, PA, Vol. 8, 1988, pp. 3–16.
20. Evans, A. G., Heuer, A. H. & Porter, D. L., The fracture toughness of ceramics. In *Proc. Fourth Int. Conf. on Fracture*, Vol. 1, 1977, ed. D. M. R. Taplin, Pergamon Press Inc., New York, p. 529.
21. Travitzky, N. A. & Claussen, N., Microstructure and mechanical properties of cordierite-ZrO₂ composites. In *Proc. Advanced Ceramics II*, ed. S. Sōmiya. Elsevier Applied Science Publishers, London 1986, pp. 121–35.